Journal of Ceramic Processing Research. Vol. 17, No. 5, pp. 434~438 (2016)

J O U R N A L O F
Ceramic Processing Research

Characterization and *in vitro* evaluation of nanostructure Barium titanate coating on Ti6Al4V

Shahram Rahmati[a], Mohammad Basir Basiriani[b], Mohammad Rafienia[c,*], Jaber Yaghini[d], Keyvan Raeissi[b], Saeid Hosseini[e] and Sattar Kabiri[f]

[a]*Department of Biomaterials, Nanotechnology and Tissue Engineering, School of Advanced Medical Technologies, Isfahan University of Medical Sciences, Isfahan, 81744176, Iran*
[b]*Department of Materials Engineering, Isfahan University of Technology, Isfahan, 84156-83111, Iran*
[c]*Biosensor Research Center, Isfahan University of Medical Sciences, Isfahan, 81744176, Iran*
[d]*Dental Implant Research Center and Department of Periodontology, School of Dentistry, Isfahan University of Medical Sciences, Isfahan, 81744176, Iran*
[e]*School of Dentistry, Isfahan University of Medical Sciences, Isfahan, 81744176, Iran*
[f]*Orthodontic Department, Dental school, Shahid Beheshti University of Medical Sciences, Tehran, 1983963113, Iran*

Osseointegration has been the concern of implantology for many years. Researchers have used various ceramic coatings for this purpose however piezoelectric ceramics (e.g. Barium titanate) are a novel field of interest. In this regard, Barium titanate ($BaTiO_3$, BTO) coating were fabricated by electrophoretic deposition (EPD) on Ti6Al4V medical alloy, using sol-gel synthesized nanometer BTO powder. Structure and morphologies were studied using X-ray diffraction (XRD) and scanning electron microscopy (SEM) respectively. Results showed homogenous coating with cubic structure and crystallite size of about 41 nm. Bioactivity response of coated samples while immersion in simulated body fluid (SBF) were evaluated by SEM and inductively coupled plasma (ICP) analysis. Cell compatibility was also studied via MTT assay and SEM imaging. SEM images indicated Apatite formation on the coating after 7 days of SBF immersion, and ICP analysis approved ions concentration decrement in SBF. Cells showed flattened morphology in intimate contact with coating after 12 h of culture. Altogether, coated samples demonstrated appropriate bioactivity and biocompatibility.

Key words: Barium titanate, Sol-gel, Electrophoretic deposition (EPD), Bioactivity, Cytotoxicity.

Introduction

Healing process in the implants is based on osseointegration that was defined as direct contact between bone and implant without microscopic defection, by Branemark et al. [1]. Minimum trauma in surgery, initial stability, and prevention of infection and micromotion are fundamental requirements for osseointegration [1]. Osseointegration and bone response in the case of formation rate, quantity, and quality of the new bone depend on implant properties [2]. Studies have shown that faster bone modeling can fix implant tightly and prevent fibrous layer formation on the surface of implant [3]. Various techniques have been used to improve bone and implant surface connection with the goal of faster integration, bone remodeling, and more implant stability during healing time, so that earlier loading could be apply [2].

Implant properties such as surface chemistry, electrical charge, surface topography, and porosity could affect bone response at *in vivo* conditions [4]. Titanium and its alloys are the most commercial alloys used for implants due to their mechanical properties, corrosion resistance, and biocompatibility [5, 6]. Different methods have been used to improve implant properties and its integration, such as different coatings like Titania, Calcium phosphate or Hydroxyapatite, as well as surface roughening or chemical modifications on the implant surface [6-9]. But another concept in this case are piezoelectric materials. They could be useful because of bone intrinsic piezoelectricity [10, 11].

Barium titanate (BTO), due to its well-known piezoelectric properties, is one of the electroactive ceramics that has the capability of being used as a bioceramic [12, 13]. Among various coating methods, Electrophoretic deposition (EPD) is a simple and inexpensive method that has interested many researchers in recent years for coating of diverse bioceramics such as hydroxyapatite [14], bioglass [15], forsterite [16] etc. Many researchers have studied EPD process for barium titanate [17-19] but no biomedical evaluation has been reported.

In this study, BTO was introduced as a novel bioceramic coating. BTO electrophoretically was coated on Ti6Al4V medical alloy and its bioactivity and cell compatibility were studied.

*Corresponding author:
Tel : +98-31-37925266
Fax: +98-31-37925274
E-mail: m_rafienia@med.mui.ac.ir

Materials and Methods

BTO powder synthesis

Equimolar amounts of barium diethoxide ($Ba(OC_2H_5)_2$, Alfa Aesar, USA), and titanium tetraisopropoxide ($Ti(OC_3H_7)_4$, Alfa Aesar, USA) were dissolved in ethylene glycol monomethyl ether (EGMME: $CH_3OC_2H_4OH$, Merck, Germany) to prepare precursor solution with the concentration of 0.25 M under dry argon atmosphere. Solution was hydrolyzed by adding water and EGMME (with a volume ratio of 1 : 1) in −17 °C for 20 min. After ageing for 24 h, the obtained gel was dried in 90 °C and heat-treated at 800 °C for 1 h.

Electrophoretic deposition

A mixture of EGMME and acetylacetone (Acac: $CH_3COCH_2COCH_3$, Merck, Germany), with a volume ratio of 9:1 was used as electrophoretic medium. BTO particles were added to the solution with a concentration of 0.2 M and agitated ultrasonically to achieve a stable suspension. Two Ti6Al4V (ASTM grade 5, Galimplant S.L., Spain) plates of 2 × 1 cm were used as electrodes with a distance of 2 cm. The specimens were prepared by grinding with silicon carbide abrasive paper up to 600 grit. A dc voltage of 60 V applied for 5 minutes. Coatings were dried in the air at 90 °C and sintered at 800 °C for 1 h.

Structural characterization

X-ray diffraction (XRD, Philips X'Pert-MPD system, Netherland) with CuK_α beam ($\lambda = 0.1543$ nm) was used for structure analysis in according to JCPD standard cards. The crystallite size of synthesized powder and coating was determined using the Scherrer equation (Equation 1):

$$t = \frac{k\lambda}{\beta \cos\theta} \quad (1)$$

Where β is the width of peak in the middle of its height, λ is the wavelength (0.154 nm), θ is the Bragg angle, k is a constant (0.9), and t is the apparent crystallite size.

Size and morphologies

The powder particle size distribution, was evaluated by dynamic light scattering (DLS, Malvern ZEN3600, UK). The morphology of coatings was investigated by scanning electron microscopy (SEM, Philips XL30, Netherland) after gold coating (about several nanometers thick) using a sputter coater (Bal-Tec, SCD 005, USA) to create surface conductivity.

Bioactivity evaluation

Bioactivity of BTO coatings was evaluated by immersing in simulated body fluid (SBF) prepared using Kokubo method [20]. After immersion for 3, 7, 14 and 28 days, specimens' surface morphology and element analysis was studied by using a SEM equipped with energy dispersive X-ray spectroscopy (EDS, SeronAIS-2100, Korea) system. Ions concentration changes also evaluated by means of inductively coupled plasma (ICP, Optima 7300DV, USA) analysis.

Cell culture

MG-63 cell-line cells were cultured in a Dulbecco's modified Eagle's medium (DMEM, Bio-Idea, Iran) containing 10% Fetal bovine serum (FBS, Bio-Idea, Iran) and 1% Penicillin/ streptomycin (Pen/strep, Bio-Idea, Iran) for several passages to reach a stable phenotype. About 10'000 cells were seeded on each sample and were incubated for 0.5, 1, 4 and 7 days. Then samples were washed with Phosphate buffered saline (PBS, Bio-Idea, Iran) to eliminate unattached cells and fixed in 2% glutaraldehyde for 30 min at room temperature. After several dehydrations in ethanol (30 min in 50%, 70%, 80%, 90% and 100% ethanol, subsequently), SEM (Philips XL30, Netherland) was used to study cells morphology on the surface.

MTT assay

For MTT assay about 10'000 cells were seeded on 1 × 1 cm coated samples and were incubated for 1, 4 and 7 days in a 24-well plate (three samples for each day). Polystyrene plate (Biofil, China) was also used as control. At appointed days after removal of culture medium, 700 µl DMEM and 70 µl 3-(4,5-dimethylthiazol-2-yl)-2,5-diphenyltetrazolium (MTT, 5 mg/ml in PBS) were added to each well and they were incubated for 3 h. Afterward, medium was removed and 700 µl Dimethyl sulfoxide (DMSO, Sigma, UK) was added to each well and they were incubated for 1 h. DMSO was removed and was added to three wells of a 96-well plate and absorbance was read using an automated plate reader (Microplate Reader Model 1680, Bio-Rad, USA) at 540 nm, subsequently. Average value and standard deviation of optical density (OD) were calculated and reported. A $p < 0.05$ was considered significant in statistical analyses using ANOVA.

Results and Discussion

Phase structure analysis

Fig. 1 shows XRD patterns of the synthesized powder and coating. According to the standard card of BTO (JCPD #01-075-0212) both of them have cubic perovskite structure. Coating shows sharper and higher peaks especially in high angles that reveals higher crystallinity. Calculated crystallite size of powder was about 25 nm whilst it was 41 nm for the coating. Furthermore, small peak transition to lower angles could be seen in almost all peaks that shows more interplanar distance. All are results of coating further sintering process that eased diffusion and made structure more crystalline.

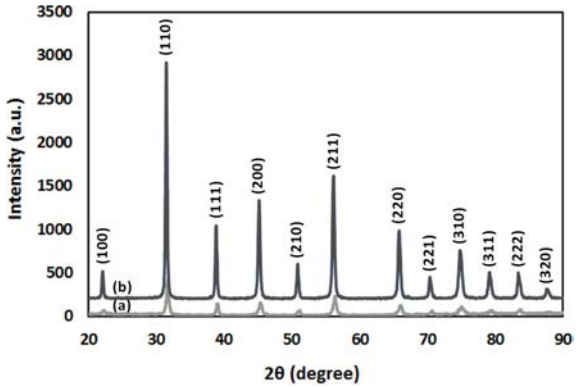

Fig. 1. X-ray diffraction patterns of BTO synthesized powder (a) and coating (b).

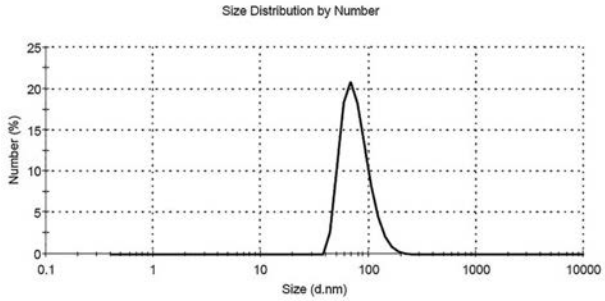

Fig. 2. Particle size distribution of synthesized nanoparticles.

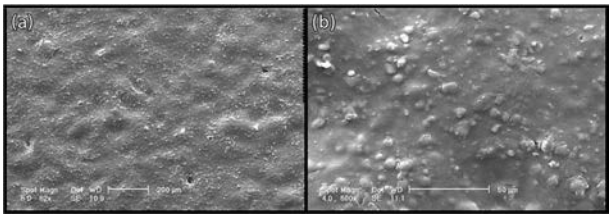

Fig. 3. SEM micrographs of BTO coating deposited by EPD under 60V/5min. (a) 60X, (b) 500X.

Particle size evaluation

DLS analysis of particles size is shown in Fig. 2. As it can be seen, particles are in the range of 40-110 nm with one peak around 70 nm. In comparison to XRD results, it seems that each particle consists of a few numbers crystallites. Li et al. [21] reached to an average size of ~10 nm via a similar synthesis method for both crystallite and particle sizes. This difference may relate to better powder dispersion, and their colder hydrolyzing temperature (–20 ºC) that provided higher activation free energy for nucleation.

Coating morphology

Fig. 3 demonstrates SEM images of the samples after sintering. Particles agglomeration is obvious with signs of substrate roughness. Micro-holes which are the cause of electrolyte evaporation during drying and some micro-crakes were inevitable. Notwithstanding the presence of these defects, coatings have had sufficient strength and adhesion to substrate.

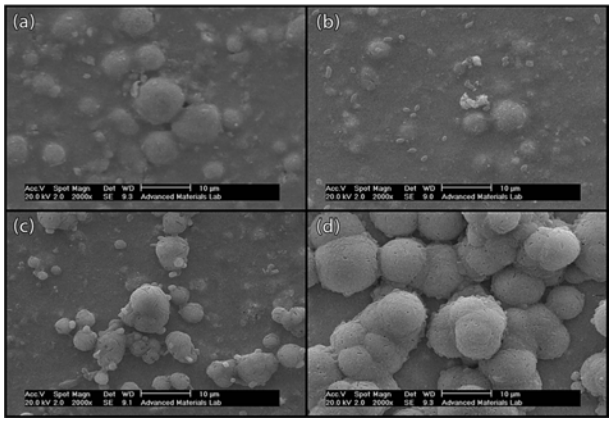

Fig. 4. SEM micrographs of BTO surface immersed in SBF after 3 (a), 7 (b), 14 (c) and 28 (d) days.

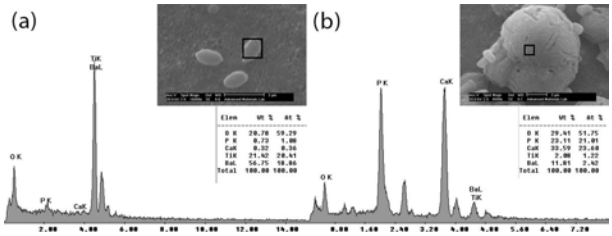

Fig. 5. EDS spectra of apatite nuclei after 7 (a) and 14 (b) days immersion in SBF.

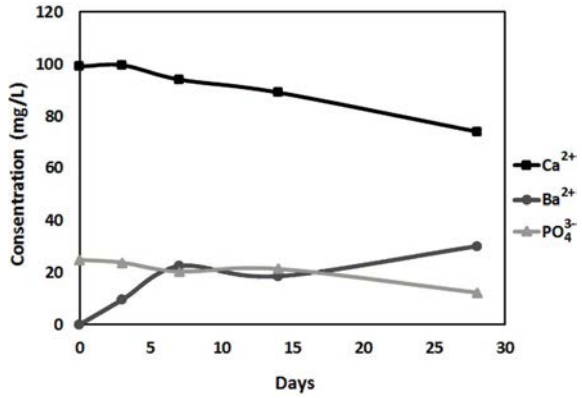

Fig. 6. SBF ions concentration changing in the presence of BTO coated samples during 4 weeks.

Bioactivity evaluation

In vitro biomineralization of the coated samples during 4 weeks immersion in SBF is shown in Fig. 4. Apatite nuclei were appeared after 7 days on the surface. Globular precipitates growth and conjugation were occurred subsequently. In addition, new nuclei are obvious on the surface of older ones after 14 and 28 days.

EDS results on 7 and 14 days samples (Fig. 5) qualified precipitates apatite chemistry while it is well known that using standardless EDS analysis do not have sufficient quantitative accuracy to determine the formula of a compound [22].

SBF ions concentration during 4 weeks of bioactivity test revealed in Fig. 6. Calcium and phosphate ions

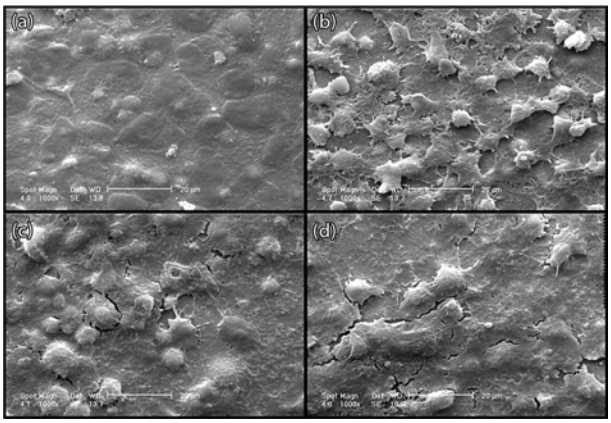

Fig. 7. MG-63 cells morphology after 0.5 (a), 1 (b), 4 (c) and 7 (d) days of culture on the surface of BTO coating.

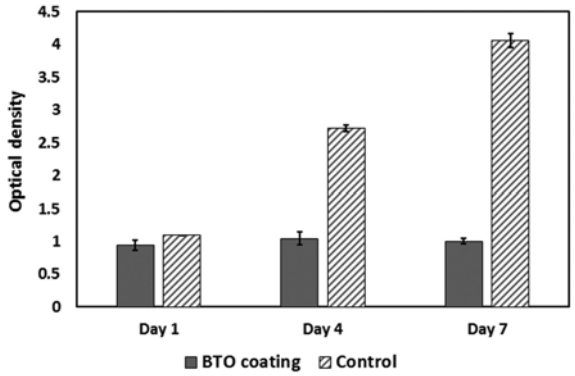

Fig. 8. MTT assay results for BTO coating and control in 1, 4 and 7 days after culture.

decreased with an increasing rate, because of growing apatites are more suitable substrates for new apatite nucleation and make precipitation faster. Difference in Ca^{2+} and PO_4^{3-} losing amount is related to apatite stoichiometry ($Ca_{10}(PO_4)_6(OH)_2$) that needs Ca^{2+} about two times more than PO_4^{3-}. In the other hand, it could be seen that Ba^{2+} leached from coating to the solution, as also have seen previously in nanometric barium titanate [23]. Nevertheless, apatite precipitates slowdown releasing rate of Ba^{2+} ions by covering the surface along with time.

Cell culture

The morphology of MG-63 cells cultured on BTO coated samples was examined using SEM. Some of the images obtained of cells cultured after 0.5, 1, 4 and 7 days are shown in Fig. 7. Cells displayed a flattened morphology in intimate contact with the coating surface after first 12 h. After 24 h, appearance of lamellipodia demonstrates cells migration on the surface [24] in order to reach to an appropriate distribution. In 4th and 7th days cells completely covered the surface and show good attachment to each other and BTO surface.

MTT assay

Fig. 8 shows MTT assay results comparing the samples and control. BTO had no statistically significant changes during 7 days whilst control showed cell proliferation. But this difference could not simply consider as a sign of cytotoxicity since cells were seen in SEM images flattened and attached to the surface. The only probable reason may be Ba^{2+} ions leaching from ceramic. Studies that have investigated composites involving BTO particles, with adequate MTT results [24, 25] have had micrometer size BTO particles. So it seems that further sintering processes could be useful to make micrometer size particles and eliminate ions leaching.

Conclusions

Ti6Al4V coated samples with BTO were fabricated by electrophoretic deposition (EPD) using synthesized nanometer BTO powders followed by sintering at 800 ºC. Morphological studies showed homogenous coating with signs of EPD medium evaporation. Bioactivity of the coated specimens were studied in SBF at 37 ºC endorsed apatite formation on the surface. Cell seeding also showed good attachment to the surface but MTT assay resulting in lack of proliferation that may be a result of ion leaching. Concluding all results shows capability of BTO coating to use as implant coating for *in vivo* applications.

Acknowledgments

The authors would like to express their appreciation to Iran National Science Foundation (INSF) for the financial support (Grant No. 91002863).

References

1. T. Berglundh, I. Abrahamsson, N.P. Lang, J. Lindhe, Clin. Oral Implants Res. 14 (2003) 251-262.
2. A.B. Jr Novaes, S.L. de Souza, R.R. de Barros, K.K. Pereira, G. Iezzi, A. Piattelli, Braz. Dent. J. 21 (2010) 471-481.
3. B. Elmengaard, J.E. Bechtold, K. Soballe, Biomaterials 26 (2005) 3521-3526.
4. D.M. Ferris, G.D. Moodie, P.M. Dimond, C.W.D. Giorani, M.G. Ehrlich, R.F. Valentini, Biomaterials 20 (1999) 2323-2331.
5. L. Sennerby, A. Dasmah, B. Larsson, M. Iverhed, Clin. Implant Dent. Relat. Res. 7 (2005) Suppl 1:S13-20.
6. G. Giavaresi, L. Ambrosio, G.A. Battiston, U. Casellato, R. Gerbasi, M. Finia, N.N. Aldini, L. Martini, L. Rimondini, R. Giardino, Biomaterials 25 (2004) 5583-5591.
7. P.R. Klokkevold, R.D. Nishimura, M. Adachi, A. Caputo, Clin. Oral Implants Res. 8 (1997) 442-447.
8. V.K. Balla, S. Banerjee, S. Bose, A. Bandyopadhyay, Acta Biomater. 6 (2010) 2329-2334.
9. L. Le Gu´ehennec, A. Soueidan, P. Layrolle, Y. Amouriq, Dental Mater. 23 (2007) 844-854.
10. E. Fukada, I. Yasuda, J. Phys. Soc. Jpn. 12 (1957) 1158.
11. A.A. Marino, R.O. Becker, Nature 228 (1970) 473-474.
12. F. Jianqing, Y. Huipin, Z. Xingdong, Biomaterials, 18 (1997) 1531-1534.
13. J.B. Park, A.F. von Recum, G.H. Kenner, B.J. Kelly, W.W.

Coffeen, M.F. Grether, J. Biomed. Mater. Res. 14 (1980) 269-277.
14. C.T. Kwok, P.K. Wong, F.T. Cheng, H.C. Man, Appl. Surf. Sci. 255 (2009) 6736-6744.
15. R. Rojaee, M.H. Fathi, K. Raeissi, M.H. Taherian, Ceram. Int. 40 (2014) 7879-7888.
16. S.N. Hosseini, H.R. Salimi Jazi, M.H. Fathi, Mater. Lett. 143 (2015) 16-19.
17. K. Raju, D.H. Yoon, Mater. Lett. 110 (2013) 188-190.
18. Y.J. Wu, J. Li, T. Koga, M. Kuwabara, J. Electroceramics, 21 (2008) 189-192.
19. A. Dogan, G. Gunkaya, E. Suvaci, M. Niederberger, Key Eng. Mater. 314 (2006) 133-140.
20. T. Kokubo, H. Takadama, Biomaterials 27 (2006) 2907-2915.
21. J. Li, Y.J. Wu, H. Tanaka, T. Yamamoto, M. Kuwabara, J. Am. Ceram. Soc. 87 (2004) 1578-1581.
22. D.E. Newbury, N.W.M. Ritchie, Scanning 35 (2013) 141-168.
23. D.H. Yoon, B.I. Lee, P. Badheka, X. Wang, J. Mater. Sci.: Mater. Electron. 14 (2003) 165-169.
24. F.R. Baxter, I.G. Turner, C.R. Bowen, J.P. Gittings, J.B. Chaudhuri, J. Mater. Sci.: Mater. Med. 20 (2009) 1697-1708.
25. L.N. Teixeira, G.E. Crippa, A.C. Trabuco, R. Gimenes, M.A. Zaghete, D.B. Palioto, P.T. de Oliveira, A.L. Rosa, M.M. Beloti, Acta Biomater. 6 (2010) 979-989.